Five *Arabidopsis* peroxin 11 homologs individually promote peroxisome elongation, duplication or aggregation

Matthew J. Lingard and Richard N. Trelease*

School of Life Sciences, Arizona State University, PO Box 874501, Tempe, AZ 85287-4501, USA

*Author for correspondence (e-mail: trelease.dick@asu.edu)

Accepted 26 January 2006
Journal of Cell Science 119, 1961-1972 Published by The Company of Biologists 2006
doi:10.1242/jcs.02904

Summary

Pex11 homologs and dynamin-related proteins uniquely regulate peroxisome division (cell-cycle-dependent duplication) and proliferation (cell-cycle-independent multiplication). *Arabidopsis* plants possess five Pex11 homologs designated in this study as *At*Pex11a, -b, -c, -d and -e. Transcripts for four isoforms were found in *Arabidopsis* plant parts and in cells in suspension culture; by contrast, *At*Pex11a transcripts were found only in developing siliques. Within 2.5 hours after biolistic bombardments, myc-tagged or GFP-tagged *At*Pex11 a, -b, -c, -d and -e individually sorted from the cytosol directly to peroxisomes; none trafficked indirectly through the endoplasmic reticulum. Both termini of myc-tagged *At*Pex11 b, -c, -d and -e faced the cytosol, whereas the N- and C-termini of myc-*At*Pex11a faced the cytosol and matrix, respectively. In *At*Pex11a- or *At*Pex11e-transformed cells, peroxisomes doubled in number. Those peroxisomes bearing myc-*At*Pex11a, but not myc-*At*Pex11e, elongated prior to duplication. In cells transformed with *At*Pex11c or *At*Pex11d, peroxisomes elongated without subsequent fission. In *At*Pex11b-transformed cells, peroxisomes were aggregated and rounded. A C-terminal dilysine motif, present in *At*Pex11c, -d and -e, was not necessary for *At*Pex11d-induced peroxisome elongation. However, deletion of the motif from myc-*At*Pex11e led to peroxisome elongation and fission, indicating that the motif in this isoform promotes fission without elongation. In summary, all five overexpressed *At*Pex11 isoforms sort directly to peroxisomal membranes where they individually promote duplication (*At*Pex11a, -e), aggregation (*At*Pex11b), or elongation without fission (*At*Pex11c, -d).

Supplementary material available online at
http://jcs.biologists.org/cgi/content/full/119/9/1961/DC1

Key words: *Arabidopsis*, Peroxisome, Proliferation, Division, Duplication, Pex11

Introduction

Peroxisomes are generally defined as relatively small (0.1-1 μm in diameter), spherical organelles bound by a single membrane. However, this definition greatly oversimplifies the pleomorphic nature of peroxisomes, which can be spherical, toric, rod-shaped, elongated/tubular, or reticular (Yamamoto and Fahimi, 1987; Schrader et al., 1994; Cutler et al., 2000; Collings et al., 2002; Mano et al., 2002; Muench and Mullen, 2003). Furthermore, internal and/or external cues might induce dramatic shifts in peroxisomal size, shape and commensurate protein composition (Huang et al., 1983; Veenhuis et al., 2000; Schrader and Fahimi, 2004; Titorenko and Rachubinski, 2004). In yeasts, plants and mammals, changes in peroxisomal biogenesis patterns are mediated by expression of peroxisome biogenesis proteins encoded by at least 32, 15 and 22 peroxin genes (*PEX*), respectively (Mullen et al., 2001; Matsumoto et al., 2003; Vizeacoumar et al., 2004; and see also tabulated information on peroxin homologs at http://lsweb.la.asu.edu/rtrelease/pdf/Tables.pdf). These genes and their corresponding protein products (PexNp) are numbered in order of their discovery (e.g. Pex1p, Pex2p, etc.) (Distel et al., 1996).

Among the 32 identified yeast peroxins, the peroxin 11-type (Pex11p) homologs, in concert with dynamin-related proteins, uniquely regulate peroxisome division and/or proliferation. Mammals, yeasts and trypanosomes each possess a 'family' of three structurally and functionally homologous isoforms of Pex11p (Thoms and Erdmann, 2005; Yan et al., 2005). In this study, we adapt terminology and definitions from Yan et al. for changes in peroxisome size, shape and number (Yan et al., 2005). For example, the process of 'peroxisome division' refers to cell-cycle-related duplication (doubling) of pre-existing peroxisomes. The process of 'peroxisome proliferation' refers to an induced, several-fold increase in size and/or number of pre-existing peroxisomes within a short time period, independent of cell-cycle peroxisome division.

Roles for Pex11p in peroxisome proliferation were identified first in *Saccharomyces cerevisiae* and *Candida boidinii pex11*Δ mutants (*Scpex11*Δ and *Cbpex11*Δ, respectively) (Marshall et al., 1995; Sakai et al., 1995). Under normal conditions, proliferation of peroxisomes 0.1-0.3 μm in diameter was induced in yeasts grown on growth medium substrates (e.g. oleate, methanol, etc.) that were at least partly metabolized in peroxisomes (Sakai and Subramani, 2000; Veenhuis et al., 2003). *Scpex11*Δ or *Cbpex11*Δ mutants grown on oleic acid

Journal of Cell Science

possessed one or two peroxisomes that were 5-10 times the size of normal oleate-induced peroxisomes (Erdmann and Blobel, 1995; Sakai et al., 1995). By contrast, overexpression of *Sc*Pex11p in wild-type, oleate-grown *S. cerevisiae* resulted in peroxisomal elongation and subsequent proliferation of normal-sized, rounded peroxisomes that filled much of the cytoplasm (Marshall et al., 1995). Two other *Sc*Pex11p homologs, *Sc*Pex25p and *Sc*Pex27p, were identified that regulated peroxisomal proliferation (Smith et al., 2002; Rottensteiner et al., 2003; Tam et al., 2003). *Sc*Pex11p, *Sc*Pex25p and *Sc*Pex27p are peripheral peroxisomal membrane proteins (PMPs) situated on the cytosolic side of the peroxisomal membrane (Marshall et al., 1995; Smith et al., 2002; Tam et al., 2003). Overproduction of a single Pex11 isoform in *Penicillium chrysogenum* resulted in proliferation of elongated/tubulated peroxisomes (Kiel et al., 2004).

Pex11 family members in mammals (e.g. *Homo sapiens*, *Mus musculus* and *Rattus norvegicus*) are named Pex11α, -β and -γ. Pex11α was identified in the liver of rats treated with clofibrate, a xenobiotic that induced peroxisome proliferation (Abe et al., 1998), whereas Pex11β was found to be constitutively expressed in most tissues (Abe and Fujiki, 1998). Overexpression of *Hs*Pex11β (and -α to a lesser degree) induced peroxisome proliferation in a multistep process in which peroxisome elongation preceded fission(s) (Schrader et al., 1998). However, *Hs*Pex11β-knockout mice exhibited embryo lethality, indicating that cell-cycle-dependent peroxisome division was aborted. Whether peroxisome division occurs subsequent to peroxisome elongation, as does peroxisome proliferation, is not well established. Another constitutively expressed mammalian Pex11 homolog (Pex11γ) was identified in the liver of mice and humans (Li et al., 2002; Tanaka et al., 2003). Overexpression of this peroxin isoform induced slight peroxisome tubulation, enlargement and clustering; however, there was no evidence for an increase in the number of peroxisomes per cell. Mouse and human Pex11 homologs are bitopic integral membrane proteins with both their N- and C-termini exposed to the cytosol (Abe and Fujiki, 1998; Abe et al., 1998; Passreiter et al., 1998; Schrader et al., 1998; Li et al., 2002).

Mammalian and yeast cells lacking the dynamin-like proteins (DLPs) DLP1 or Vsp1p possessed fewer peroxisomes that were enlarged/elongated relative to wild-type cells (Hoepfner et al., 2001; Koch et al., 2003; Li and Gould, 2003). Overexpression of the same DLPs in wild-type yeast and mammalian cells did not induce changes in peroxisome size and number. Koch et al. (Koch et al., 2004) showed that knockdown of DLP1 resulted in elongated peroxisomes, suggesting that it was necessary for peroxisome fission. Overexpression of Pex11β in these cells induced further peroxisome elongation, but did not induce fissions. Furthermore, they determined that peroxisomal constriction (preceding fission) occurred independent of both Pex11β and DLP1 expression.

The only plant protein known to participate in the regulation of plant peroxisome proliferation and/or division is the *Arabidopsis* dynamin-related protein 3A (DRP3A). Mano et al. showed that peroxisomes in cells of transgenic plants lacking DRP3A were elongated, suggesting that normal peroxisome division was impaired (Mano et al., 2004). In wild-type cells, they found that overexpressed DRP3A localized on the cytosolic surface of the peroxisomal membrane did not induce changes in peroxisomal morphology and/or number per cell.

Inducible changes in plant peroxisomal number and morphology have been documented in plants. Morré et al. and Oksanen et al. demonstrated that Norway spruce, aspen and birch trees exposed to ozone exhibited peroxisome proliferation (doubling in spruce, 26-47% increase in aspen, and 38% increase in birch) (Morré et al., 1990; Oksanen et al., 2003). Palma et al. reported that treatment of pea plants with clofibrate induced peroxisome proliferation (approximate quadrupling) (Palma et al., 1991). Pais and Feijó noted that peroxisomes in developing pollen grains of *Ophrys lutea* increased in size and number per cell, forming an interconnected body of spherical peroxisomes (Pais and Feijó, 1987). In *Lemna minor* fronds, Ferreira et al. observed that fission of elongated peroxisomes correlated with exposure to increased light levels (Ferreira et al., 1989). Collings et al. observed horseshoe- and dumbbell-shaped peroxisomes at the cell plate within the phragmoplast of dividing onion-root meristem cells (Collings et al., 2003). Kunce et al. documented elongation of glyoxysomes in cotyledons of growing cottonseed seedlings (Kunce et al., 1984). Significantly, no efforts were made in any of these studies to identify molecular elements or machinery related to these proliferative events. Also noteworthy is the virtual absence of data pertaining to division (duplication) of plant peroxisomes for constitutive cell division.

The intent of this current study was to identify in protein databases potential *Arabidopsis* Pex11 (*At*Pex11) homolog(s), identify the subcellular sorting pathway of transiently overexpressed *At*Pex11 protein(s), and determine whether these overexpressed proteins promoted changes in peroxisome morphology and/or number per cell. Transcripts of the five *Arabidopsis PEX11* genes (*AtPEX11a*, *-b*, *-c*, *-d* and *-e*) were detected in *Arabidopsis* plant parts; notably, transcripts of *AtPEX11a* were detected only in developing siliques (seed pods). All five myc-tagged Pex11 proteins individually sorted directly to the boundary membrane of *Arabidopsis* suspension cell peroxisomes. Peroxisomes bearing overexpressed individual myc-*At*Pex11 proteins exhibited isoform-specific peroxisome morphological and/or numerical changes: elongation without subsequent fission (division and/or proliferation) (*At*Pex11c and -d); elongation prior to duplication (*At*Pex11a); duplication without prior elongation (*At*Pex11e); and apparent aggregation without fission or elongation (*At*Pex11b). These general interpretations are discussed in terms of amino acid similarities and differences between the *At*Pex11 isoforms, and the presence and functional influence of the C-terminal dilysine motif within *At*Pex11c, -d and -e.

Results

Identification and sequence comparisons of five *Arabidopsis* Pex11 proteins

BLAST searches (TAIR protein database; http://www.arabidopsis.org/Blast/) for *C. boidinii* Pex11p (*Cb*Pex11p) homologs revealed the existence of five putative *Arabidopsis* Pex11 proteins: At1g47750, At3g47430, At1g01820, At2g45740 and At3g61070, corresponding to *At*Pex11a, -b, -c, -d and -e, respectively. All five exhibited 20-24% amino acid sequence identity with *Cb*Pex11p and 18-25%

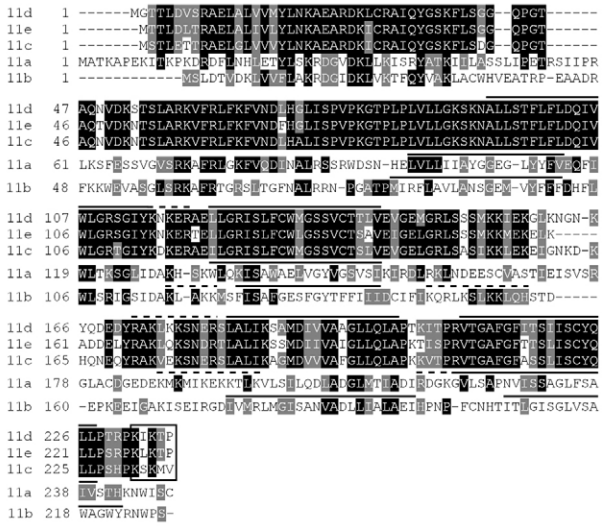

Fig. 1. Amino acid sequence alignment of *At*Pex11a, -b, -c, -d and -e. *At*Pex11 protein sequences were aligned using the ClustalW algorithm (http://www.ch.embnet.org/software/ClustalW.html). Identical and similar residues were shaded black and gray, respectively, with BOXSHADE (http://www.ch.embnet.org/software/BOX_form.html). Transmembrane domains were predicted using TMpred (http://www.ch.embnet.org/software/TMPRED_form.html), and are overlined in black. Basic clusters of amino acid residues are overlined with dashes. Dilysine motifs are boxed.

amino acid sequence identity with human *Hs*Pex11α and -β. *At*Pex11a was the only putative peroxin homolog identified in a BLAST search against *Hs*Pex11γ; conversely, only *At*Pex11c, -d and -e were identified in BLAST searches against *Sc*Pex11p. No *At*Pex11 homologs were identified when *Sc*Pex25p, *Sc*Pex27p or *Trypanosoma brucei* Pex11p (*Tb*Pex11p) were used to search the TAIR protein database.

The amino acid sequence alignment in Fig. 1 shows that *At*Pex11c, -d and -e are highly similar to each other (75% average identity and 92% average similarity), whereas *At*Pex11a and -b are less similar to *At*Pex11c, -d and -e (22% average identity and 44% average similarity). *At*Pex11a and -b exhibit 31% identity and 51% similarity to each other. The *At*Pex11 proteins possess at least three (*At*Pex11a) or four (*At*Pex11b, -c, -d and -e) predicted transmembrane domains (TMDs) (Fig. 1, solid lines). PMPs characteristically possess a peroxisomal membrane-targeting signal (mPTS) comprising a TMD near a basic cluster of amino acid residues. Each *At*Pex11p sequence possesses at least two basic clusters of amino acid residues (Fig. 1, dashed lines) that might constitute a portion of a mPTS; these putative mPTSs on *At*Pex11c, -d and -e share high similarity. *At*Pex11c, -d and -e each possess a C-terminal dilysine motif.

Transcripts for all five *AtPEX11* genes exist in *Arabidopsis* plant parts (organs) and suspension cells

Non-quantitative reverse transcriptase (RT)-PCR was employed to determine which, if any, of the putative *At*Pex11 isoforms were expressed in *Arabidopsis* developing siliques (seed pods), roots, leaves and/or suspension culture cells. Fig. 2 shows that four of the five *AtPEX11* gene transcripts (approximately 700 bp in length) are expressed in roots, leaves

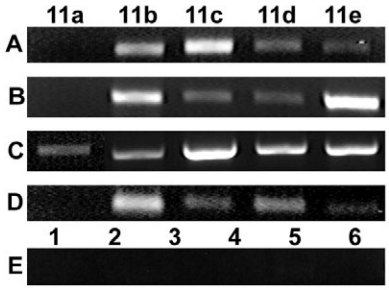

Fig. 2. Gene transcripts of *AtPEX11a*, *-b*, *-c*, *-d* and *-e* are expressed in *Arabidopsis* roots, leaves, siliques and suspension culture cells. Total RNA extracted from 5-week-old roots (A), leaves (B) and developing siliques (seed pods) (C), or 3-day-cultured suspension cells (D), was treated with DNase I and reverse transcribed using poly-T primers. *AtPEX11a*, *-b*, *-c*, *-d* and *-e* (labeled here 11a-11e) were amplified by PCR using primers complimentary to 5′ or 3′ termini. Control reactions (E) were designed using the following noncomplementary primer pairs in a leaf cDNA library: foreword primers for *AtPEX11c* (lanes 1,2), *AtPEX11d* (lanes 3,4) and *AtPEX11e* (lanes 5,6), and reverse primers for *AtPEX11d* (lanes 1,6), *AtPEX11e* (lanes 2,4) and *AtPEX11c* (lanes 3,5). No PCR products were observed for any of these reactions. PCR products, shown here, were separated electrophoretically in a 1% agarose gel containing ethidium bromide. As expected, all PCR products were approximately 700 bp in length.

and suspension culture cells, but *At*Pex11a transcripts were not. However, transcripts for all five genes were detected in silique RNA extracts. Because of the high degree of similarity among *AtPEX11c*, *-d* and *-e*, control PCRs were employed in which foreword primers for one *AtPEX11* gene (e.g. *AtPEX11c*) were paired with reverse primers from another *AtPEX11* gene (e.g. *AtPEX11d*). Leaf RNA was used for the control PCRs. No PCR product was produced from any of these control reactions (Fig. 2E, lanes 1-6).

Transiently expressed myc-*At*Pex11 homologs sort directly from the cytosol to peroxisomes in *Arabidopsis* and tobacco BY-2 suspension cells

Shortly after biolistic bombardments, transformed cells were examined by (immuno)fluorescence microscopy to determine the sorting pathway and subcellular localization(s) of each overexpressed myc- or GFP-tagged *At*Pex11 protein. The earliest time point that proteins were consistently visualized within transformed cells was 2.5 hours post-bombardment. Panels A, F, K and P in Fig. 3 show in each transformed *Arabidopsis* (Fig. 3A,F) or BY-2 (Fig. 3K,P) cell a punctate fluorescence pattern resulting from dual immunolabeling with anti-myc plus Cy-2-conjugated (anti-myc/Cy-2) antibodies (Fig. 3A,K) and anti-catalase plus RhodamineX-conjugated (anti-catalase/RhodamineX) (Fig. 3F,P) antibodies. In both cell types, myc-tagged *At*Pex11a colocalized with endogenous catalase in peroxisomes (arrowheads); by contrast, myc-tagged *At*Pex11a was not observed in any other organelles (e.g. endoplasmic reticulum; ER) at any time point. The general morphology of the peroxisomes in these transformed cells is the same as the morphology of peroxisomes in neighboring nontransformed cells, i.e. rounded (spherical) or rod-shaped (Fig. 3, arrows). Comparisons of these panels also illustrate that peroxisomes in *Arabidopsis* cells are characteristically

larger and fewer in number per cell than peroxisomes in BY-2 cells.

Arabidopsis and BY-2 cells overexpressing each of the other four myc-*At*Pex11 proteins also exhibited colocalizations with endogenous peroxisomal catalase (compare Fig. 3B-E with G-J; and L-O with Q-T). None of these Pex11 proteins was detected in any other organellar compartment. Notably, peroxisomes in approximately 50% of transformed cells possessing myc-*At*Pex11c or myc-*At*Pex11d at 2.5 hours were distinctly elongated in *Arabidopsis* (Fig. 3C,D) and BY-2 (Fig. 3M,N) cells. Virtually all of the cells transformed with myc-*At*Pex11a, -b or -e at 2.5 hours possessed normal peroxisomes that were spherical-to-rod shaped, similar to those in surrounding, nontransformed cells (e.g. Fig. 3G,P-T). In parallel experiments, GFP-*At*Pex11a, -c and -d also sorted directly to peroxisomes at early hours (data not shown).

Peroxisomes with overexpressed myc-*At*Pex11c or -d elongate whereas peroxisomes bearing myc-*At*Pex11b aggregate

Our visual observations that *Arabidopsis* peroxisomes bearing myc-*At*Pex11c or -d were somewhat elongated within about 50% of the transformed cells at 2.5 hours (Fig. 3C,D) prompted further examination of peroxisomes in these and other myc-*At*Pex11-transformed cells at later time points. For a cell-transformation and time-course control, *Arabidopsis* cells were bombarded with a gene encoding chloramphenicol acetyltransferase (CAT) with an appended C-terminal type 1 peroxisomal matrix-targeting signal (CAT-SKL). Peroxisomes in these transformed cells were used to derive a range of shapes and sizes for non-induced peroxisomes throughout a gene expression period of 72 hours. This was the longest time period that cells could be maintained without adverse effects of contamination, nutrient deprivation, etc.

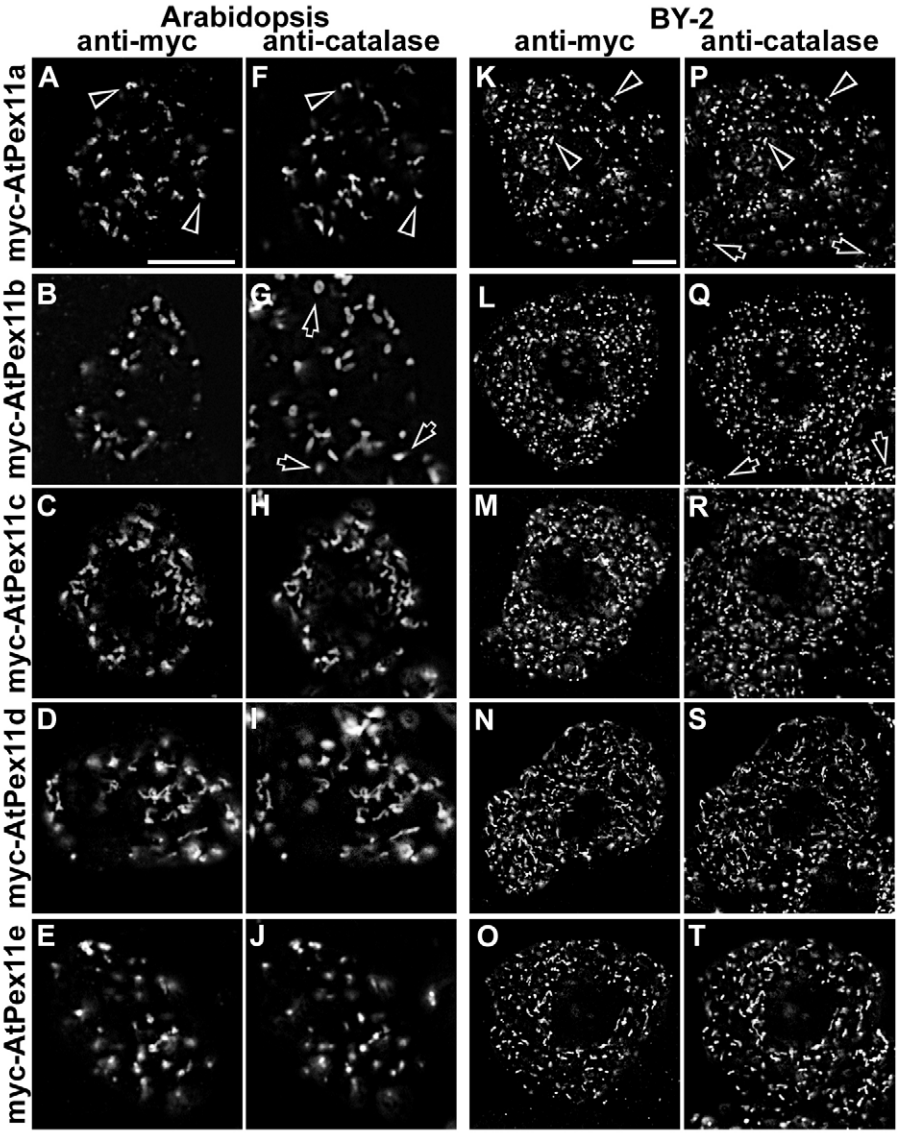

Fig. 3. Immunofluorescence images illustrate that overexpressed, myc-tagged *At*Pex11a, -b, -c, -d and -e sort directly to peroxisomes during a 2.5 hour post-bombardment period in dual immunolabeled *Arabidopsis* and tobacco BY-2 suspension cells. The five myc-tagged *At*Pex11 proteins were introduced individually (biolistic bombardments) into *Arabidopsis* (A-J) or BY-2 (K-T) cells. Following bombardments (2.5 hours), cells were fixed in formaldehyde, cell walls perforated/digested with pectolyase (and cellulase, *Arabidopsis* only), and membranes permeabilized in Triton X-100. Cells were then dual immunolabeled with anti-myc plus anti-Cy-2-conjugated antibodies (1:500; 1 hour each) and anti-catalase plus RhodamineX-conjugated antibodies (1:2000; 1 hour each) (labeled columns of cells). Each representative image depicts one transformed cell per panel (labels on left side). In all cases, the myc-*At*Pex11 protein is colocalized with peroxisomal catalase (arrowheads point to examples in A,F,K,P). Arrows point to peroxisomes in neighboring nontransformed cells. Bars, 10 μm.

Fig. 4A-P (upper panels) shows representative micrographs of peroxisomes in single transformed cells bearing overexpressed myc-*At*Pex11c, -d, -b and CAT-SKL at 24, 48 and 72 hours post-bombardment. Peroxisomes that acquired myc-*At*Pex11c (Fig. 4A-D) or -d (Fig. 4E-H) became elongated/tubulated and remained as such through 72 hours. Visual comparisons of these 5-10 μm long peroxisomes with the 1-3 μm long peroxisomes within neighboring wild-type (Fig. 4B,F; arrowheads) or CAT-SKL-transformed cells (Fig. 4M-P) revealed the extent of peroxisomal elongation in myc-*At*Pex11c-transformed cells and myc-*At*Pex11d-transformed cells. Insets with higher magnifications of peroxisomes facilitate these visual comparisons. A dramatically different morphological effect was observed for peroxisomes that acquired myc-*At*Pex11b (Fig. I-L). All of these peroxisomes assumed a spherical/toric shape, which appeared to be a consequence of peroxisome aggregation.

Fig. 4Q (bottom panel) shows the percentage of *At*Pex11-

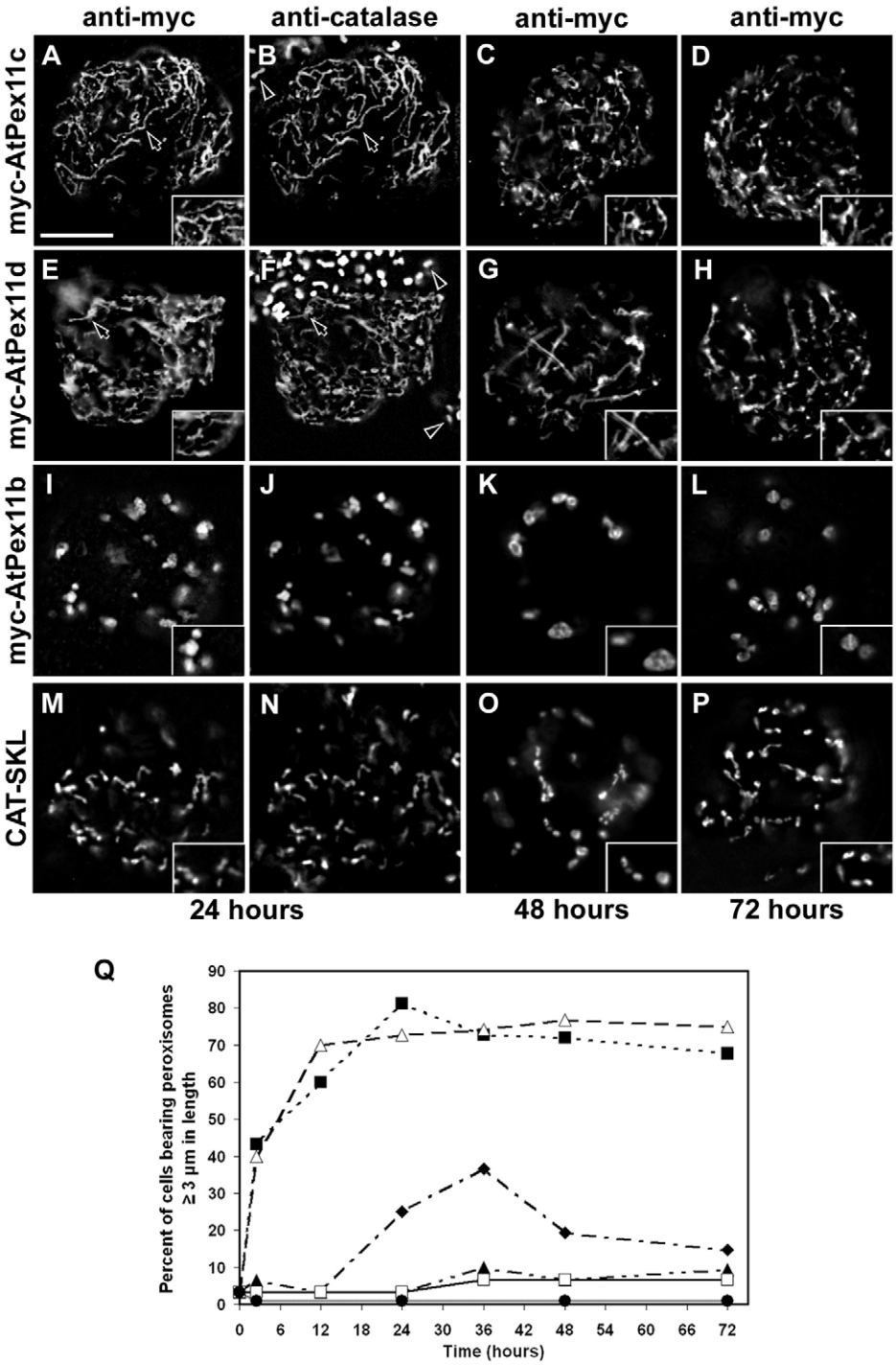

Fig. 4. *Arabidopsis* peroxisomes bearing overexpressed myc-*At*Pex11c and -d became elongated/tubulated (2.5-72 hours), whereas peroxisomes acquiring myc-*At*Pex11b became spherical. (A-H) A representative single transformed cell in each panel illustrates elongated peroxisomes possessing myc-*At*Pex11c (A,C,D) or myc-*At*Pex11d (E,G,H). Arrows point to examples of perfect colocalization between these myc-tagged proteins (A,E) and endogenous peroxisomal catalase (B,F). Arrowheads point to normal spherical or rod-shaped peroxisomes in neighboring nontransformed cells. (I-L) Single representative transformed cells show spherical/toric peroxisomes bearing overexpressed myc-*At*Pex11b (I,K,L) perfectly colocalized with endogenous peroxisomal catalase (compare I and J). (M-P) Peroxisomes bearing CAT-SKL (M,O,P) are spherical or rod-shaped and are perfectly colocalized with endogenous catalase (compare M and N). (Q, lower panel) Graphical representation of the percentage of transformed cells bearing peroxisomes ⩾3 μm at various time points post-bombardment (n⩾30 for all data points). Cells were bombarded with myc-*AtPEX11a* (◆), -*b*(●), -*c* (■), -*d* (△), -*e* (▲) or *CAT-SKL* (□), fixed at the indicated time points (x-axis), and immunolabeled with anti-myc plus Cy-2-conjugated antibodies or anti-CAT plus Cy-2-conjugated antibodies. Intercepts at the y-axis (0 hours) were projected to the baseline (3% elongation) for each construct. Bar, 10 μm.

transformed cells possessing elongated (⩾3 μm long) peroxisomes at various time points. Fewer than 5% of peroxisomes in cells transformed with CAT-SKL were elongated during the entire gene expression time period (2.5-72 hours). None of the peroxisomes in cells transformed with myc-*At*Pex11b was elongated at any time. A nearly constant low percentage (5-10%) of cells transformed with myc-*At*Pex11e possessed elongated peroxisomes. A dramatic difference was apparent in cells transformed with myc-*At*Pex11c or -d. As noted earlier, at 2.5 hours post-bombardment, approximately 50% of the transformed cells possessed elongated peroxisomes. Within 12 hours, approximately 60-70% of cells transformed with myc-*At*Pex11c or -d possessed elongated peroxisomes. Throughout the rest of the time course, essentially the same percentage (⩾70%) of these transformed cells possessed elongated peroxisomes. Cells transformed with myc-*At*Pex11a exhibited a significant difference in the degree of peroxisome elongation. Only a small percentage (approximately 5%) of these transformed cells possessed elongated peroxisomes up to 12 hours. Thereafter, the percentage increased to a peak of 37% at 36 hours followed by a gradual decline to about the same level as CAT-SKL-transformed cells.

Similar overexpression experiments were carried out with untagged versions of *At*Pex11a, -d and -e. The same morphological results were observed at 24 and 48 hours post-bombardment for each isoform, indicating that the myc epitope tag did not influence peroxisome morphology (Fig. S1, supplementary material).

Peroxisomes bearing myc-*At*Pex11a and -e increase in number per cell between 5 and 72 hours

Fig. 5A illustrates that myc-*At*Pex11a-bearing peroxisomes observed at 5 hours post-bombardment are mostly spherical or rod shaped. However, at 24 hours, peroxisomes in about 25% of the transformed cells possess clearly elongated peroxisomes (Fig. 5B). These observations are consistent with data presented in Fig. 4Q. At 45 hours, a striking difference was observed in virtually all of the transformed cells on the microscope slides; peroxisomes in these cells were mostly spherical and visibly more numerous (compare Fig. 5C to 5A and Fig. 3A). Similar images of spherical, proliferated peroxisomes were observed in myc-*At*Pex11a-transformed cells at 72 hours (data not shown).

At 5 and 24 hours, peroxisomes bearing myc-*At*Pex11e were rounded/rod shaped (Fig. 5D,E and Fig. 4Q) and exhibited approximately the same number of peroxisomes per cell as cells expressing CAT-SKL (Fig. 5I,J). Notably, at 24 hours, the peroxisomes were not elongated. At 45 hours, virtually all transformed cells on the microscope slides possessed visibly proliferated, rounded peroxisomes (compare Fig. 5F to 5D), which is remarkably similar to the myc-*At*Pex11a-proliferated peroxisomes (compare Fig. 5F to 5C). A similar apparent increase in the number of rounded peroxisomes was evident when cells were transformed with a GFP-*At*Pex11e construct (Fig. 5G,H). At 24 hours, the autofluorescent rounded/rod-shaped peroxisomes bearing this chimeric protein apparently were less numerous than they were at 72 hours (compare Fig. 5G to 5H). Fig. 5I,J illustrates that peroxisomes bearing CAT-SKL (Fig. 5I) and endogenous catalase (Fig. 5J) are colocalized and are rounded/rod shaped at 45 hours, like those bearing myc- or GFP-*At*Pex11e at 24 hours (Fig. 5E,G). The number of peroxisomes in the CAT-SKL-transformed cell is visibly less than the number of peroxisomes in the cells transformed with myc- or GFP-*At*Pex11e (45 and 72 hours; Fig. 5F,H) or myc-*At*Pex11a (24 and 45 hours; Fig. 5B,C).

These microscopic observations prompted numerical analyses of the perceived peroxisomal multiplications observed in *At*Pex11-transformed cells (Table 1). Cells transiently transformed with the CAT-SKL construct were used to establish baseline values for peroxisome number in transformed cells at 24, 45 and 72 hours post-bombardment. The number of CAT-SKL-bearing peroxisomes remained virtually constant (8-9 peroxisomes per 100 μm^2) at the three time points (Table 1). At 24 hours, the number of peroxisomes bearing myc-*At*Pex11e conformed to the baseline value, whereas the number of those bearing myc-*At*Pex11a was approximately double the baseline value (17 peroxisomes per 100 μm^2). At 45 hours, the number of peroxisomes possessing either myc-*At*Pex11e or myc-*At*Pex11a was approximately doubled (17-19 peroxisomes per μm^2). The number of myc-*At*Pex11e-bearing peroxisomes did not change during the next 27 hours of expression (72 hours post-bombardment). An Independent Samples T Test confirmed that there was a significant

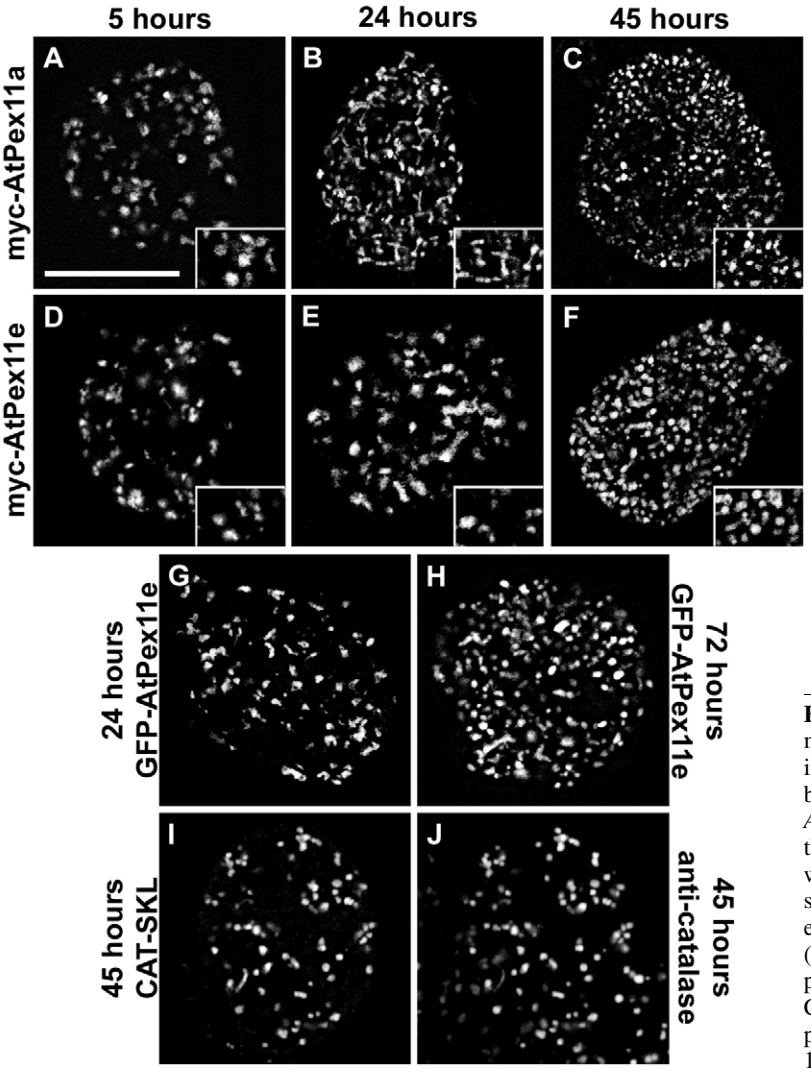

Fig. 5. *Arabidopsis* peroxisomes bearing overexpressed myc-*At*Pex11a, myc-*At*Pex11e or GFP-*At*Pex11e increase in number per cell between 5 and 45 hours post-bombardment. (A-F, upper panels) Representative myc-*At*Pex11-transformed cells (left side labels) were fixed at three time points (top labels) and then dual immunolabeled with anti-myc plus Cy-2-conjugated (and anti-catalase, not shown) antibodies. (G-J, lower panels) Single cells expressing chimeric proteins (left and right side labels). (G,H) GFP autofluorescent peroxisomes at 24 and 72 hours post-bombardment. (I,J) Peroxisomal colocalization of anti-CAT/Cy-2 (I) and anti-catalase/Cy-5 (J) antibodies. All panels are confocal epifluorescence projection images. Bar, 10 μm.

Table 1. Numerical analyses of the peroxisomal multiplications observed in *At*Pex11-transformed cells

Gene construct	Hours expression	*Peroxisomes per 100 μm^2
CAT-SKL	24	8.14±0.32
myc-*AtPEX11e*	24	9.87±0.44
myc-*AtPEX11a*	24	16.79±0.57
CAT-SKL	45	8.86±0.25
myc-*AtPEX11e*	45	18.83±0.46
myc-*AtPEX11a*	45	17.05±0.31
CAT-SKL	72	9.80±0.31
myc-*AtPEX11e*	72	19.23±0.41
GFP-*AtPEX11e*	72	18.91±0.44

Peroxisomal acquisition of overexpressed *At*Pex11a or *At*Pex11e induces a doubling (twofold increase) in the number of peroxisomes in *Arabidopsis* cells. For each gene construct, peroxisomes in 30 transformed cells were examined by laser-scanning confocal microscopy (4-8 optical sections per cell, 2 μm between each section) and the number of peroxisomes in optical sections of each transformed cell was enumerated using MetaMorph v6.1. The *CAT-SKL* construct was a non-induction transformation control for the autofluorescent GFP- and myc-tagged *PEX11* constructs.

*Values are mean ± s.e.m.

difference (P<0.001) between the mean number of peroxisomes per 100 μm^2 in cells transformed with *At*Pex11a (24 and 48 hours) or *At*Pex11e (48 and 72 hours) compared with cells transformed with CAT-SKL. There was no significant difference between the numbers of peroxisomes in cells transformed with CAT-SKL at the different time points. To validate the statistically significant doubling of myc-*At*Pex11e-bearing peroxisomes at 72 hours, cells were transformed with GFP-*At*Pex11e. Table 1 shows that the number of GFP-*At*Pex11e-bearing peroxisomes was approximately double the baseline value.

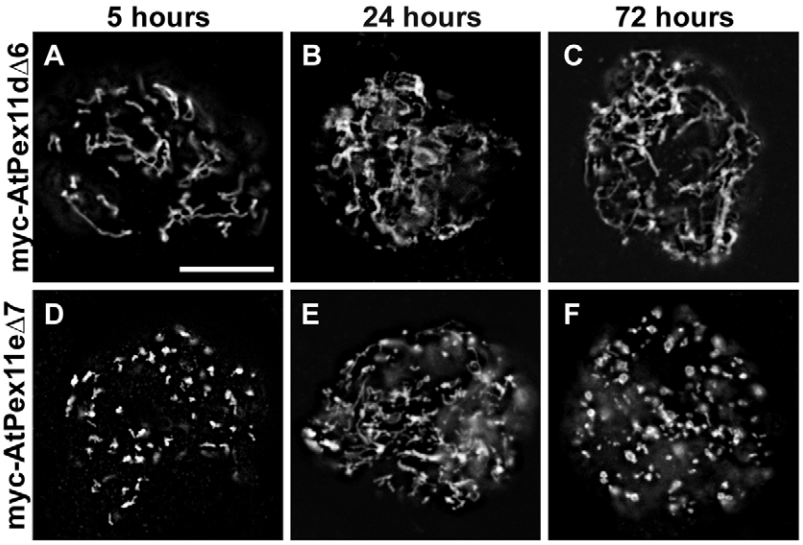

Fig. 6. Deletion of the C-terminal dilysine motif in *At*Pex11d and -e (myc-*At*Pex11dΔ6 or -eΔ7, respectively) variously affected changes in *Arabidopsis* peroxisome morphology and duplication. Cells transformed with myc-*At*Pex11dΔ6 (A-C) or myc-*At*Pex11eΔ7 (D-F) were fixed at three time points (top labels) and immunolabeled with anti-myc plus Cy-2-conjugated antibodies(dual label with anti-catalase not shown). Bar, 10 μm.

Influence of the C-terminal dilysine motifs in myc-*At*Pex11d and myc-*At*Pex11e on peroxisomal elongation and duplication

To determine whether the C-terminal dilysine motif was necessary for myc-*At*Pex11-induced peroxisomal elongation and/or duplication, myc-*At*Pex11dΔ6 and myc-*At*Pex11eΔ7 constructs that lacked their dilysine motifs were produced. At 5, 24 and 72 hours, peroxisomes bearing myc-*At*Pex11dΔ6 were elongated (Fig. 6A-C), as were peroxisomes bearing the wild-type protein (Fig. 4E,H). Conversely, peroxisomes bearing myc-*At*Pex11eΔ7 exhibited a time-dependent change in morphology not observed for peroxisomes bearing myc-*At*Pex11e. At 5 hours, peroxisomes bearing myc-*At*Pex11eΔ7 were rounded/rod shaped (Fig. 6D) similar to peroxisomes bearing the wild-type protein (Fig. 5D). At 24 hours, peroxisomes bearing myc-*At*Pex11eΔ7 were elongated, unlike the rounded peroxisomes bearing the wild-type protein construct (compare Fig. 6E to Fig. 5E and Fig. 4Q). At 72 hours, myc-*At*Pex11eΔ7-bearing peroxisomes were no longer elongated, but were rounded and visibly increased in number per cell (Fig. 6F) similar to *At*Pex11e-bearing peroxisomes at 45 or 72 hours (Fig. 5F). Hence, unlike peroxisomes in cells transformed with myc-*At*Pex11e, those in cells transformed with myc-*At*Pex11eΔ7 elongated prior to duplication (compare Fig. 5D-F with Fig. 6D-F).

Topological orientation of peroxisomal myc-*At*Pex11 proteins in vivo

To determine the topological orientation of peroxisomal myc-*At*Pex11 proteins in vivo, digitonin was applied to permeabilize plasma, but not peroxisomal, membranes of cells transformed with genes encoding C- or N-terminal myc-tagged *At*Pex11a, -b, -c, -d or -e. Fig. 7A,C-J shows fluorescence from peroxisomes in individual myc-labeled cells transformed with each of the genes. Notably, no fluorescence was observed in cells transformed with *At*Pex11a-myc (Fig. 7B). As expected, variations in peroxisome morphology and number were apparent among the different transformed cells; hence, appendage of the myc epitope to the N- or C-terminus did not produce variant peroxisomal morphology. Fig. 7K-T shows results of anti-catalase/Rhodamine fluorescence labeling in the same dual immunolabeled cells depicted in Fig. 7A-J. In all cases, anti-catalase/Rhodamine fluorescence signals from the transformed cells were not observed, indicating that anti-catalase IgGs were not accessible to the peroxisomal matrix. Combined, these results indicated that the N-termini of each myc-tagged *At*Pex11 homolog and the C-termini of *At*Pex11b, -c, -d or -e immunoreacted with anti-myc antibodies present in the cytosol only.

The myc-*At*Pex3 protein was expressed in *Arabidopsis* cells as a control to verify that a N-terminal myc epitope tag facing the peroxisomal matrix was inaccessible to anti-myc/Cy-2 antibodies in digitonin-treated cells; this orientation for myc-*At*Pex3p was shown previously in BY-2 cells (Hunt and Trelease, 2004). Fig. 7U,V shows that transformed cells

permeabilized with digitonin and dual immunolabeled with anti-myc/Cy-2 and anti-catalase/Rhodamine antibodies exhibit no (peroxisomal) fluorescence. Confirmation of myc-*At*Pex3p expression in transformed cells is shown in Fig. 7W,X where anti-myc/Cy-2- and anti-catalase/Rhodamine-labeled peroxisomes are visualized in samples from the same batch of cells permeabilized with Triton X-100. As another positive control for digitonin permeabilization, cells from the same myc-*At*Pex3p transformation experiment were incubated in digitonin and dual immunolabeled with anti-tubulin plus Cy-2-conjugated (endogenous microtubules) and anti-catalase/Rhodamine antibodies. Immunofluorescence images of cortical microtubules in the cytoplasm (Fig. 7Y), but not of peroxisomal matrix catalase (Fig. 7Z) confirmed that incubation in digitonin permeabilized plasma and not peroxisomal membranes.

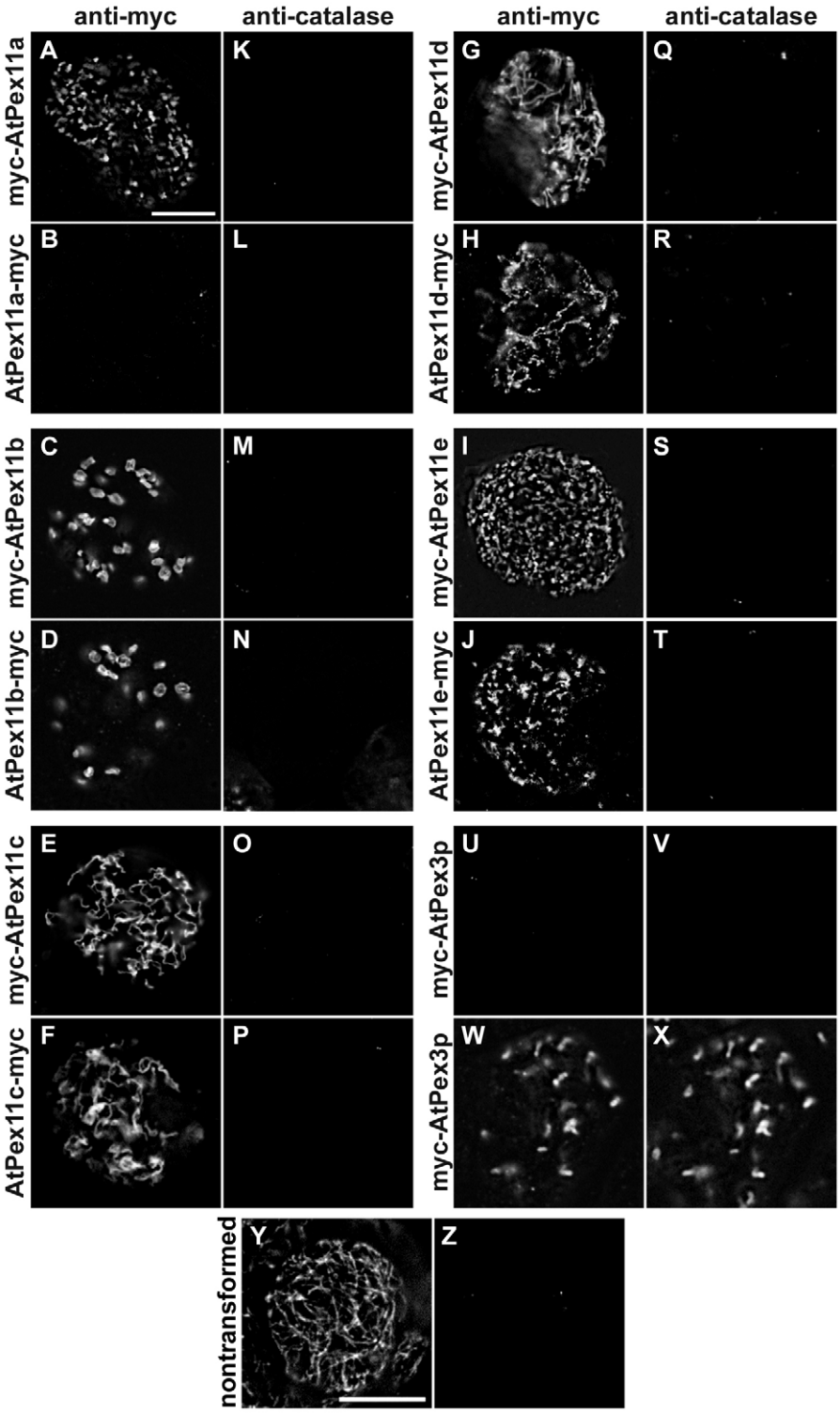

Fig. 7. Both the C- and N-termini of *At*Pex11b, -c, -d and -e are on the cytosolic side of the peroxisomal membrane, whereas the N- and C-termini of *At*Pex11a are on the cytosolic and matrix side of the membrane, respectively. (A-T) Bombarded cells were fixed in formaldehyde at 24 (C-H) or 48 (A,B,I,J) hours, treated with pectinase, and then incubated in digitonin to permeabilize plasma (not organellar) membranes. Labels on the left of each pair of panels indicate myc-tagged proteins dual immunolabeled with anti-myc (A-U) and anti-catalase antibodies (K-V). (U-Z) Controls for digitonin permeabilization. (U-X) Anti-myc plus Cy-2-conjugated (U,W) and anti-catalase plus RhodamineX-conjugated (V,X) antibodies applied to cells transformed with myc-*At*Pex3p and permeabilized with digitonin (U,V) or Triton X-100 (W,X). (Y,Z) A cell from the same batch of *At*Pex3p-transformed cells permeabilized with digitonin and dual immunolabeled with anti-tubulin plus Cy-2-conjugated (Y) and anti-catalase plus Rhodamine-conjugated (Z) antibodies. Bars, 10 μm.

Discussion

The presence of *AtPEX11b*, *-c*, *-d* and *-e* gene transcripts in all *Arabidopsis* parts examined suggests that these four *At*Pex11 gene products participate constitutively in peroxisomal biogenesis throughout the plant body. This premise, of course, is conditional upon whether *At*Pex11 proteins are expressed constitutively in these cells. This information was not acquired because of our lack of specific antibodies raised against each of the isoforms. The presence of *AtPEX11a* gene transcripts only in developing siliques suggests that *AtPEX11a* expression is involved in seed development.

Multiple TMDs are predicted to occur in each of the *At*Pex11 isoforms (Fig. 1), similar to their mammalian and yeast homologs that are integrally and peripherally associated PMPs, respectively (Marshall et al., 1995; Abe and Fujiki, 1998; Abe et al., 1998; Passreiter et al., 1998; Schrader et al., 1998; Li et al., 2002; Smith et al., 2002;

Tam et al., 2003). Not surprisingly, our findings from differential permeabilization experiments showed that the N- and C-termini of myc-tagged *At*Pex11b, -c, -d and -e faced the cytosol (Fig. 7), indicating that these four proteins were associated with the peroxisomal boundary membrane where they promoted varied changes in peroxisome morphology. The membrane topology of *At*Pex11a is unique among Pex11 isoforms in all organisms, i.e. the N- and C-termini are situated on opposite faces of the *Arabidopsis* peroxisomal membrane, indicative of an integral membrane association. The significance of this topological difference is unknown.

Intracellular trafficking of *At*Pex11 isoforms

PMPs are divided into two groups based on their post-translational sorting pathway (Titorenko and Rachubinski, 2001; Trelease, 2002). Group I PMPs sort indirectly through the ER from their site of synthesis in the cytosol to forming or pre-existing peroxisomes, whereas group II PMPs sort directly to peroxisomes. Both groups of PMPs have been identified and characterized in plant cells (Trelease and Lingard, 2006). Although immunofluorescence signals from some of the myc-tagged *At*Pex11 isoforms were observed in the cytosol of some cells at early time points, there was no evidence for localization in any ER-like organelle before their appearance in pre-existing peroxisomes (Fig. 3). Therefore, we conclude that all five myc-*At*Pex11 isoforms are group II PMPs. We are unaware of any group I Pex11 homolog in other organisms.

Peroxisome multiplication

In mammalian cells, a generalized sequential process for Pex11-induced peroxisome proliferation entails: (1) Pex11p insertion into the peroxisome membrane, (2) peroxisome elongation, (3) Pex11p segregation from other PMPs, and (4) peroxisome segmentation and fission into numerous new peroxisomes (Schrader et al., 1998; Koch et al., 2004). Evidence for a similar process [e.g. elongation preceding fission(s)], was also found in *S. cerevisiae* and *P. chrysogenum* (Marshall et al., 1995; Kiel et al., 2004). Marshall et al. observed elongated clusters of budding (dividing) peroxisomes in cells overexpressing *Sc*Pex11p (Marshall et al., 1995). Hoepfner et al. reported that peroxisomes in cells lacking the dynamin-like protein *Sc*Vps1p elongated without fission(s), resulting in cells with a single elongated peroxisome (Hoepfner et al., 2001). Other studies, however, suggest that peroxisome proliferation in *S. cerevisiae* does not adhere to this generalized process. For example, overexpression of *Sc*Pex11p, -25p, or -27p resulted in proliferation of numerous peroxisomes without notable elongation (Rottensteiner et al., 2003; Tam et al., 2003; Vizeacoumar et al., 2003; Vizeacoumar et al., 2004). Hence, fission(s) of elongated peroxisomes is not yet firmly established as a generalized process for multiplication of pre-existing peroxisomes.

*At*Pex11e-induced peroxisome duplication seemingly does not adhere to the generalized mammalian process. Specifically, fewer than 10% of cells transformed with myc-*At*Pex11e were observed to possess elongated peroxisomes at multiple time points through 72 hours (Fig. 4Q), indicating that myc-*At*Pex11e did not induce peroxisome elongation. However, if one considers the combined presence of transcripts for *At*Pex11c, -d and -e in wild-type *Arabidopsis* suspension cells (Fig. 2), then an alternative interpretation for the role of *At*Pex11e in peroxisome division emerges. Prior to, or during, cell-cycle-dependent cell division, spherical peroxisomes (1 μm diameter) might elongate into rod-shaped structures (3 μm in length) in response to *At*Pex11c and/or *At*Pex11d, and then divide into spherical peroxisomes in response to *At*Pex11e. These daughter peroxisomes would then segregate into daughter cells.

The identification of elongated peroxisomes in cells overexpressing *At*Pex11a further implicates elongation in the duplication process of *Arabidopsis* peroxisomes. Up to 36% of cells bearing myc-*At*Pex11a possessed elongated peroxisomes through 36 hours post-bombardment. It may be that, as for *At*Pex11c and *At*Pex11d, this peroxin induces peroxisome elongation (nearly) simultaneously with peroxisome duplication. If fission occurs more rapidly than elongation, then no elongated peroxisomes would be present, as was observed in *At*Pex11e-transformed cells. If, by contrast, peroxisome elongation outpaces fission, then at least some elongated peroxisomes would be in evidence, but not to the same degree as observed in cells transformed with *At*Pex11c and *At*Pex11d. These considerations offer a plausible explanation for the lower percentage of elongated peroxisomes in *At*Pex11a-transformed cells compared with the substantially higher percentage in *At*Pex11c- or *At*Pex11d-transformed cells.

Peroxisome proliferation versus division

Definitive evidence for Pex11 involvement in cell-cycle-regulated peroxisome division within actively dividing cells is limited in all organisms. In an early study, *Hs*Pex11β was implicated in the constitutive control of peroxisomal abundance owing to its uniform expression in various rat tissues and unchanged mRNA levels in tissues treated with peroxisome proliferating agents (Schrader et al., 1998). In another study, Pex11β-knockout mice exhibited neonatal lethality (Li et al., 2002). Their cells possessed peroxisomes that were slightly elongated and less numerous per cell, further implying that Pex11β was necessary for normal peroxisome division.

In this study, separate overexpression of two *At*Pex11 isoforms (*At*Pex11a and *At*Pex11e) promoted an approximate doubling in number of pre-existing peroxisomes. Of the two isoforms, transcripts for only *At*Pex11e were expressed in multiple plant parts, implying that it promotes peroxisome division in constitutively dividing plant cells. That overexpression of *At*Pex11a and *At*Pex11e uniquely promotes duplication of peroxisomes, rather than proliferation as observed upon overexpression of mammalian Pex11 isoforms, is also suggestive of a role for these plant peroxins in cell-cycle-associated division of pre-existing peroxisomes. As noted, however, the evidence at this time is indirect.

Peroxisome elongation

*At*Pex11c and *At*Pex11d uniquely promote peroxisome elongation without associated division and proliferation; no other Pex11 homolog in any organism has been shown to promote only peroxisome elongation. In plant cells, there are numerous examples of terminal peroxisome elongation at different stages of growth and development. Specifically, peroxisomes in cotyledon cells of germinated oilseed seedlings, greening leaves and developing root nodules all undergo dramatic increases in spherical or cylindrical volume, but do not

increase in number (Gruber et al., 1973; Wanner and Theimer, 1978; Kunce et al., 1984; Newcomb et al., 1985). Exposure of *Arabidopsis* suspension cells to ultraviolet (UV) irradiation induces extensive peroxisomal elongation without subsequent multiplication (proliferation) (our unpublished observations). In HepG2 mammalian cells exposed to UV irradiation and H_2O_2, similar peroxisomal elongation/tubulation occurs without subsequent division or proliferation (Schrader et al., 1999). It might be that the results that we observed with overexpression of *At*Pex11c and/or *At*Pex11d reflected this prevalent peroxisome morphology established in plants for accomplishing dynamic metabolic fluctuations.

Within this context, induced peroxisome proliferation in some instances might be manifested as a peroxisome elongation/tubulation phenomenon without an increase in peroxisome number. Two examples are the following. In *Arabidopsis* cells, the active sites for ascorbate peroxidase and monodehydroascorbate peroxidase, two members of a peroxisome antioxidant system, are located on opposite sides of the peroxisome membrane (Lisenbee et al., 2005). This topological orientation requires that reactive oxygen substrates (H_2O_2 or ascorbate free radical) diffuse across the peroxisome membrane to interact with either enzyme. Thus, elongated peroxisomes with their increased membrane-to-matrix surface area ratio would enhance accessibility of these substrates to the enzymes. In *P. chrysogenum*, overexpression of *Pc*Pex11p, which produces elongated clusters of peroxisomes, enhances penicillin production twofold without a commensurate change in enzyme levels in the penicillin biosynthetic pathway (Kiel et al., 2004). They attributed this to the increased surface-to-volume ratio of the organelles.

Peroxisome aggregation

Remarkably consistent peroxisome morphology was observed in cells transformed with *At*Pex11b (Fig. 4). The rounded peroxisomal images were interpreted to be aggregates of peroxisomes bearing *At*Pex11b. Similar homotypic peroxisome aggregates were observed in cells overexpressing a fusion protein of ascorbate peroxidase and GFP (Lisenbee et al., 2003b). It was shown that aggregation resulted from homodimerization of the GFP moiety protruding from the boundary membranes of neighboring peroxisomes. Peroxisomes in cells transformed with a monomeric GFP variant did not form aggregates. Interestingly, homo- and hetero-oligomerization of Pex11 isoforms have been described in yeasts and trypanosomes (Maier et al., 2001; Rottensteiner et al., 2003; Tam et al., 2003). It seems reasonable to speculate that the apparent aggregates observed in *At*Pex11b-transformed cells resulted from homo-oligomerization of *At*Pex11b protruding from the *Arabidopsis* peroxisomal boundary membrane. Clusters or aggregates of rounded and/or elongated peroxisomes bearing Pex11 isoforms have also been observed in yeasts, trypanosomes and mammals (e.g. Marshall et al., 1995; Lorenz et al., 1998; Li et al., 2002).

Dilysine motif

*At*Pex11c, d and -e, like *Hs*- and *Rn*Pex11α and *Tb*Pex11p (Passreiter et al., 1998; Maier et al., 2000), possess C-terminal dilysine motifs (-KxKxx-COOH or KKxx-COOH), whereas *Arabidopsis* Pex11a and -b, like mammalian Pex11β and -γ, do not. Observations that peroxisomes bearing myc-*At*Pex11d and myc-*At*Pex11dΔ6 are elongated suggest that the motif is not necessary for peroxisomal elongation. The dilysine motifs in rat and trypanosomal, but not human, Pex11 homologs bind coatomer (COPI) subunits (Passreiter et al., 1998; Maier et al., 2000), though the functional significance of COPI binding by Pex11 homologs is unclear. Furthermore, Maier et al. reported that Pex11 proteins with mutated dilysine motifs could induce peroxisomal proliferation, similar to our results that show duplicated peroxisomes bearing myc-*At*Pex11eΔ7 (Maier et al., 2000). In summary, the dilysine motif in Pex11 does not seem to be necessary for elongation in myc-*At*Pex11d, nor does it have any effect on peroxisome division in myc-*At*Pex11e, but apparently functions somehow to prevent peroxisomal elongation.

Perspective

Several modes of action might be envisaged for Pex11-induced peroxisome elongation, division, and/or proliferation. In one scenario, one or more *PEX11* gene transcripts are expressed or activated and the protein products are targeted directly to the peroxisomal membrane where they mechanically induce peroxisome elongation with or without associated fission(s). In another scenario, one or more Pex11 protein products are targeted to the peroxisomal membrane and recruit other proteins that mechanically induce peroxisome elongation with or without associated fission(s). There is ample evidence for the latter scenario. For example, in mammals and trypanosomes, Pex11 proteins recruit COPI to the peroxisomal membrane. In mammals and yeasts, Pex11 seems to act in concert with, and/or recruit, various dynamin-like proteins (Hoepfner et al., 2001; Koch et al., 2003; Li and Gould, 2003; Koch et al., 2004). In plants, the dynamin-related protein 3A is necessary for peroxisomal division (Mano et al., 2004); however, a relationship with Pex11 protein(s) has yet to be assessed. Herein, we show that four of the five *Arabidopsis* Pex11 proteins are functional plant Pex11 homologs that can either induce peroxisome fission (duplication) with or without prior elongation, or peroxisome elongation alone. The integrated (synergistic) function(s) of these homologs with other proteins in plant cells remains to be established.

Materials and Methods

Enzymes and reagents used for DNA/RNA isolations and manipulations were obtained from BioRad, Eppendorf, Fermentas, New England Biolabs, Promega and Qiagen. Custom oligonucleotide primers were obtained from Genetech Biosciences or Integrated DNA Technologies. Plasmid cloning and whole-plasmid mutagenic reactions were verified by automated dye-terminator cycle sequencing (Arizona State University DNA Laboratory, Tempe, AZ). Gene sequences and primer designs used in this study are available upon request from the authors.

Reverse-transcriptase PCR

Expression of *AtPEX11* transcripts in *Arabidopsis* leaves, roots and suspension cells was detected by reverse transcriptase (RT)-PCR. Total RNA was isolated using the Qiagen RNeasy Plant Mini Kit and treated with DNase I. Full-length *AtPEX11* transcripts were amplified using the Promega Access RT-PCR System; oligo (dT) primers were used for the RT reaction and mutagenic primers complimentary to 5′ and 3′ ends of the *AtPEX11* transcripts were added for PCR. Products of RT-PCR experiments were separated in 1% agarose gels containing ethidium bromide and imaged with a UVP GDS-8000 System bioimaging system (Upland). The intron-free At1g47750 RT-PCR product (*AtPEX11a*) was amplified from genomic DNA using mutagenic primers that replaced the start codon with an in-frame *Xba*I restriction enzyme (RE) site and added an *Xba*I RE site after the stop codon. This product was subcloned into pCR2.1 using the Invitrogen TOPO TA Cloning Kit and sequenced.

Plasmid preparation

cDNAs encoding *AtPEX11* genes were obtained from the *Arabidopsis* Biological

Resource Center (Columbus, OH) (At3g47430-U15712), Riken (At2g45740-RAFL07-14-A08) (Seki et al., 1998; Seki et al., 2002), and D. Rhoads (Arizona State University, Tempe, AZ) (At1g01820 and At3g61070).

Full-length *AtPEX11* cDNAs were subcloned into pRTL2, a plant expression vector with a double 35S promoter, possessing the coding sequence for either an N-terminal myc epitope tag (pRTL2-Nmyc), a C-terminal myc epitope tag (pRTL2-Cmyc), or an N-terminal monomeric GFP (pRTL2-GFP_m) (Lisenbee et al., 2003b). cDNAs subcloned into pRTL2-Nmyc were PCR-amplified with mutagenic primers complimentary to 5′ and 3′ termini of *AtPEX11b*, *-c*, *-d* and *-e* designed to replace start codons with in-frame RE sites (*Bam*HI for *AtPEX11b*, *-d* and *-e*; *Xba*I for *AtPEX11c*) and to add RE sites after existing stop codons (*Xba*I for *AtPEX11c*, *-d* and *-e*; *Nhe*I for *AtPEX11b*). Constructs of *AtPEX11b*, *-d* and *-e* subcloned into pRTL2-Cmyc were amplified first with mutagenic primers that replaced stop codons with in-frame *Bam*HI RE sites and that added adjacent *Bam*HI RE sites upstream of start codons. Constructs subcloned into pRTL2-GFP_m were amplified first with primers designed to replace start codons with in-frame *Xba*I RE sites and to append in-frame *Xba*I RE sites downstream of stop codons. Following PCR amplification, all constructs were subcloned into pCR2.1 using the TOPO TA Cloning Kit. For ligation reactions, pCR2.1-*AtPEX11a*, *-b*, *-c*, *-d*, *-e* and pRTL2 plasmids were digested with the corresponding REs. Full-length *AtPEX11* DNA fragments were isolated electrophoretically in agarose gels, purified using the Qiagen QIAquick Gel Extraction Kit, and ligated to RE-digested pRTL2 vectors. pRTL2 vectors digested with one RE (e.g. *Bam*HI or *Xba*I) were treated with calf intestinal alkaline phosphatase to prevent re-circularization of plasmid DNA.

To prepare *AtPEX11a*, *-d* and *-e* constructs without epitope tags, cDNAs for each were amplified from pRTL2/*myc-AtPEX11a*, *-d* and *-e*. Mutagenic primers complimentary to 5′ and 3′ termini were used for PCRs that appended *Bam*HI RE sites upstream and adjacent to the start codons, and *Xba*I RE sites downstream and adjacent to the stop codons. PCR products were purified by agarose gel electrophoresis, digested with corresponding REs, and ligated into *Bam*HI/*Xba*I-digested pRTL2ΔNS.

myc-*At*Pex11dΔ6 and myc-*At*Pex11eΔ7 were created using the Stratagene QuikChange site-directed mutagenesis kit to replace codons $_{691}$CCC$_{693}$ (myc-*At*Pex11dΔ6) and $_{673}$CGC$_{675}$ (myc-*At*Pex11eΔ7) with stop codons (TGA).

Cell culture and microprojectile bombardment

Arabidopsis (*Arabidopsis thaliana* var. Landsberg *erecta*; a gift from S. Neill, University of West England, Bristol, UK) and tobacco BY-2 (*Nicotiana tabacum* L., cv. Bright Yellow 2) suspension cultures were maintained in MS salt and vitamin mixture (Invitrogen) and in MS salt mixture (Invitrogen), respectively. *Arabidopsis* and BY-2 cultures were propagated as described by Lisenbee et al. (Lisenbee et al., 2003a) and Banjoko and Trelease (Banjoko and Trelease, 1995), respectively, except that the 125 ml culture flasks plugged with cotton stoppers were replaced with long-necked 125 ml culture flasks capped with plastic or stainless steel caps to improve cell culture aeration and uniformity of growth.

Biolistic bombardments were carried out essentially as described by Mullen et al. (Mullen et al., 1999). Briefly, cells were collected by centrifugation 4 days after subculture (5 ml packed cell volume), resuspended aseptically in approximately 0.75 volumes transformation medium (growth medium without 2,4-D, plus 250 mM sorbitol and 250 mM mannitol) (Banjoko and Trelease, 1995; Lee et al., 1997), and incubated at room temperature, in darkness, with rocking inversion for 20 minutes. The cell suspension (4 ml) was distributed ‘drop-wise’ onto the center area (5 cm diameter circle) of three stacked, pre-moistened filter papers (Whatman #4) placed in the lid of a 10 cm Petri dish. These cells were incubated for equilibration at room temperature for 1 hour in darkness. Plasmid DNA was precipitated onto BioRad M-17 tungsten particles essentially as described by Banjoko and Trelease (Banjoko and Trelease, 1995), except that sonication for 1 minute was added as a part of each isopropanol wash to improve *Arabidopsis* suspension cell transformation efficiency. The tungsten-DNA particles were spread on the center of BioRad macrocarriers and placed in a desiccator for 20-30 minutes before bombardment. The prepared cells were biolistically bombarded in a BioRad PDS-1000/He with 10 μg plasmid DNA (two bombardments per plate), 28 inches Hg vacuum, and 1350 p.s.i. as described by Lee et al. (Lee et al., 1997).

(Immuno)fluorescence microscopy and peroxisome quantification

At intervals between 2.5 and 72 hours post-bombardment, all cells on each plate were scraped into 4% formaldehyde (prepared from paraformaldehyde; Ted Pella) in transformation medium and fixed for 1 hour at room temperature. To permit IgG diffusion into cells, cell walls were perforated/digested for 2 hours at 28°C in 0.1% (w/v) Pectolyase Y-23 (Karlan Enzymes) and 0.1% (w/v) cellulase RS (Karlan Enzymes; *Arabidopsis* cells only) diluted in phosphate-buffered saline (PBS; 140 mM NaCl, 2.7 mM KCl, 4.3 mM Na_2HPO_4, 4.4 mM KH_2PO_4, pH 7.4). Cells were then immunolabeled according to Lisenbee et al. (Lisenbee et al., 2003a). Briefly, cells were permeabilized for 15 minutes in a final concentration of 0.33% (v/v) Triton X-100 (Sigma) and then incubated with PBS-diluted primary and dye-conjugated secondary antibodies. For differential permeabilization of plasma (not peroxisomal) membranes, *Arabidopsis* cells were transformed and fixed in formaldehyde as above, but were perforated/digested in 0.1% pectinase (Sigma) for 1.5 hours at 28°C and then incubated in 25 mg/ml digitonin at room temperature for 15 minutes as described by Lisenbee et al. (Lisenbee et al., 2005).

Primary antibody sources and concentrations in PBS were as follows: mouse anti-myc monoclonal antibody 9E10 (1:500) (Santa Cruz Biotechnology), mouse anti-chick brain α-tubulin monoclonal antibody MDM1A (1:500) (Accurate Chemical and Scientific), rabbit anti-cottonseed catalase affinity-purified (protein A-Sepharose) IgGs (1:2000) (Kunce et al., 1988). Cy-2-, Cy-5- and RhodamineX-conjugated secondary antibodies were purchased from Jackson ImmunoResearch Laboratories and used in PBS at concentrations of 1:500, 1:500 and 1:2000, respectively.

Immunolabeled cells were resuspended in one volume of n-propyl gallate (10 mg/ml; Sigma) on glass slides, coverslipped, flattened with stacked weights (non-confocal epifluorescence microscopy only), and imaged as described by Hunt and Trelease (Hunt and Trelease, 2004). Images were deconvoluted using MetaMorph software (Universal Imaging) and adjusted for brightness and contrast with Adobe Photoshop 7.0 software (Adobe Systems).

Experiments and procedures to quantify the percentage of transformed cells bearing elongated peroxisomes were carried out as follows. Cells transformed individually with all five myc-*AtPEX11* or *CAT-SKL* DNA constructs were fixed in formaldehyde at 2.5, 12, 24, 36, 48 or 72 hours post-bombardment and prepared for immunofluorescence microscopy as described above. For each batch of cells transformed with myc-*AtPEX11a*, *-c*, *-d*, *-e* or *CAT-SKL*, fluorescence images (anti-myc/Cy-2 or anti-CAT/Cy-2) were acquired for at least 30 of the transformed cells. For cells transformed with myc-*AtPEX11b*, images were obtained for a minimum of 10 cells at 2.5, 24, 48 and 72 hours. Peroxisomes ⩾3 μm in length were considered elongated based on measurements made with control CAT-SKL images. Scoring of at least one elongated peroxisome per transformed cell was accomplished with a 3 μm circular template.

Experiments and procedures designed to quantify peroxisome number within *Arabidopsis* cells were carried out as follows. Transiently transformed cells prepared for immunofluorescence microscopy as described above were imaged with a Lecia Laser-Scanning Confocal Microscope. Fluorescent (anti-myc/Cy-2, GFP, or anti-catalase/Cy-5) optical sections were acquired at 2 μm intervals for each of 30 transformed cells per gene construct. Using MetaMorph v. 6.1 image-processing software, montage images were prepared from serial sections of anti-catalase/Cy-5 antibody fluorescence from each transformed cell and ‘depixelated’ (Low Pass function). The number of peroxisomes per cell optical section was computed using the following procedure: (1) cell boundaries were outlined, (2) image threshold was adjusted to highlight peroxisomal fluorescence, and (3) the number of peroxisomes per 100 μm^2 was computed and recorded. Peroxisomes were counted in 150-200 cell sections per gene construct (e.g. myc-*AtPEX11e*). The numbers of peroxisomes in cells transformed with various *AtPEX11* and *CAT-SKL* gene constructs were compared using an Independent Samples T Test to determine whether the difference between the samples was significant. SPSS software was used to derive descriptive statistics.

We thank S. Bingham for advice and directions in molecular biology aspects, D. Rhoads for cDNAs (*At*Pex11c and -e) and discussions, R. Roberson for expert guidance and suggestions on image acquisition and presentation, E. Chase Lingard for insightful assistance with statistical analyses, and H. Gustafson and T. McCartney for cell culture maintenance. *At*Pex11b was provided by the *Arabidopsis* Biological Resource Center. Support for this work was provided by National Science Foundation grant MCB-0091826 and the William N. and Myriam Pennington Foundation.

References

Abe, I. and Fujiki, Y. (1998). cDNA cloning and characterization of a constitutively expressed isoform of the human peroxin Pex11p. *Biochem. Biophys. Res. Commun.* **252**, 529-533.

Abe, I., Okumoto, K., Tamura, S. and Fujiki, Y. (1998). Clofibrate-inducible, 28-kDa peroxisomal integral membrane protein is encoded by PEX11. *FEBS Lett.* **431**, 468-472.

Banjoko, A. and Trelease, R. N. (1995). Development and application of an in vivo plant peroxisome import system. *Plant Physiol.* **107**, 1201-1208.

Collings, D. A., Harper, J. D. I., Marc, J., Overall, R. L. and Mullen, R. T. (2002). Life in the fast lane: actin-based motility of plant peroxisomes. *Can. J. Bot.* **80**, 430-441.

Collings, D. A., Harper, J. D. L. and Vaughn, K. C. (2003). The association of peroxisomes with the developing cell plate in dividing onion root cells depends on actin microfilaments and myosin. *Planta* **218**, 204-216.

Cutler, S. R., Ehrhardt, D. W., Griffitts, J. S. and Somerville, C. R. (2000). Random GFP::cDNA fusions enable visualization of subcellular structures in cells of *Arabidopsis* at a high frequency. *Proc. Natl. Acad. Sci. USA* **97**, 3718-3723.

Distel, B., Erdmann, R., Gould, S. J., Blobel, G., Crane, D. I., Cregg, J. M., Dodt, G., Fujiki, Y., Goodman, J. M., Just, W. W. et al. (1996). Unified nomenclature for peroxisome biogenesis factors. *J. Cell Biol.* **135**, 1-3.

Erdmann, R. and Blobel, G. (1995). Giant peroxisomes in oleic acid-induced *Saccharomyces cerevisiae* lacking the peroxisomal membrane protein Pmp27p. *J. Cell Biol.* **128**, 509-523.

Ferreira, R. M. B., Bird, B. and Davies, D. D. (1989). The effect of light on the structure and organization of *Lemna* peroxisomes. *J. Exp. Bot.* **40**, 1029-1035.

Gruber, P., Becker, W. and Newcomb, E. (1973). The development of microbodies and peroxisomal enzymes in greening bean leaves. *J. Cell Biol.* **56**, 500-518.

Hoepfner, D., van den Berg, M., Philippsen, P., Tabak, H. F. and Hettema, E. H. (2001). A role for Vps1p, actin, and the Myo2p motor in peroxisome abundance and inheritance in *Saccharomyces cerevisiae*. *J. Cell Biol.* **155**, 979-990.

Huang, A. H. C., Trelease, R. N. and Moore, T. S. (1983). *Plant Peroxisomes*. New York: Academic Press.

Hunt, J. E. and Trelease, R. N. (2004). Sorting pathway and molecular targeting signals for the *Arabidopsis* peroxin 3. *Biochem. Biophys. Res. Commun.* **314**, 586-596.

Kiel, J. A. K. W., van der Klei, I. J., van den Berg, M. A., Bovenberg, R. A. L. and Veenhuis, M. (2004). Overproduction of a single protein, Pc-Pex 11p, results in 2-fold enhanced penicillin production by *Penicillium chrysogenum*. *Fungal Genet. Biol.* **42**, 154-164.

Koch, A., Thiemann, M., Grabenbauer, M., Yoon, Y., McNiven, M. A. and Schrader, M. (2003). Dynamin-like protein 1 is involved in peroxisomal fission. *J. Biol. Chem.* **278**, 8597-8605.

Koch, A., Schneider, G., Luers, G. H. and Schrader, M. (2004). Peroxisome elongation and constriction but not fission can occur independently of dynamin-like protein 1. *J. Cell Sci.* **117**, 3995-4006.

Kunce, C. M., Trelease, R. N. and Doman, D. C. (1984). Ontogeny of glyoxysomes in maturing and germinated cotton seeds-a morphometric analysis. *Planta* **161**, 156-164.

Kunce, C. M., Trelease, R. N. and Turyle, R. B. Purification and biosynthesis of cottonseed (*Gossypium hirsufum L*) catalase. *Biochem. J.* **251**, 147-155.

Lee, M. S., Mullen, R. T. and Trelease, R. N. (1997). Oilseed isocitrate lyases lacking their essential type 1 peroxisomal targeting signal are piggybacked to glyoxysomes. *Plant Cell* **9**, 185-197.

Li, X. and Gould, S. J. (2003). The dynamin-like GTPase DLP1 is essential for peroxisome division and is recruited to peroxisomes in part by PEX11. *J. Biol. Chem.* **278**, 17012-17020.

Li, X., Baumgart, E., Dong, G. X., Morrell, J. C., Jimenez-Sanchez, G., Valle, D., Smith, K. D. and Gould, S. J. (2002). PEX11 alpha is required for peroxisome proliferation in response to 4-phenylbutyrate but is dispensable for peroxisome proliferator-activated receptor alpha-mediated peroxisome proliferation. *Mol. Cell. Biol.* **22**, 8226-8240.

Lisenbee, C. S., Heinze, M. and Trelease, R. N. (2003a). Peroxisomal ascorbate peroxidase resides within a subdomain of rough endoplasmic reticulum in wild-type *Arabidopsis* cells. *Plant Physiol.* **132**, 870-882.

Lisenbee, C. S., Karnik, S. K. and Trelease, R. N. (2003b). Overexpression and mislocalization of a tail-anchored GFP redefines the identity of peroxisomal ER. *Traffic* **4**, 491-501.

Lisenbee, C., Lingard, M. J. and Trelease, R. N. (2005). *Arabidopsis* peroxisomes possess functionally redundant membrane and matrix isoforms of monodehydroascorbate reductase. *Plant J.* **43**, 900-914.

Lorenz, P., Maier, A. G., Baumgart, E., Erdmann, R. and Clayton, C. (1998). Elongation and clustering of glycosomes in *Trypanosoma brucei* overexpressing the glycosomal Pex11p. *EMBO J.* **17**, 3542-3555.

Maier, A. G., Schulreich, S., Bremser, M. and Clayton, C. (2000). Binding of coatomer by the PEX11 C-terminus is not required for function. *FEBS Lett.* **484**, 82-86.

Maier, A., Lorenz, P., Voncken, F. and Clayton, C. (2001). An essential dimeric membrane protein of trypanosome glycosomes. *Mol. Microbiol.* **39**, 1443-1451.

Mano, S., Nakamori, C., Hayashi, M., Kato, A., Kondo, M. and Nishimura, M. (2002). Distribution and characterization of peroxisomes in *Arabidopsis* by visualization with GFP: dynamic morphology and actin-dependent movement. *Plant Cell Physiol.* **43**, 331-341.

Mano, S., Nakamori, C., Kondo, M., Hayashi, M. and Nishimura, M. (2004). An *Arabidopsis* dynamin-related protein, DRP3A, controls both peroxisomal and mitochondrial division. *Plant J.* **38**, 487-498.

Marshall, P. A., Krimkevich, Y. I., Lark, R. H., Dyer, J. M., Veenhuis, M. and Goodman, J. M. (1995). Pmp27 promotes peroxisomal proliferation. *J. Cell Biol.* **129**, 345-355.

Matsumoto, N., Tamura, S. and Fujiki, Y. (2003). The pathogenic peroxin Pex26p recruits the Pex1p-Pex6p AAA ATPase complexes to peroxisomes. *Nat. Cell Biol.* **5**, 454-460.

Morré, D. J., Selldén, G., Ojanperä, K., Sandelius, A. S., Egger, A., Morré, D. M., Chalko, C. M. and Chalko, R. A. (1990). Peroxisome proliferation in Norway spruce induced by ozone. *Protoplasma* **155**, 58-65.

Muench, D. G. and Mullen, R. T. (2003). Peroxisome dynamics in plant cells: a role for the cytoskeleton. *Plant Sci.* **164**, 307-315.

Mullen, R. T., Lisenbee, C. S., Miernyk, J. A. and Trelease, R. N. (1999). Peroxisomal membrane ascorbate peroxisdase is sorted to a membranous network that resembles a subdomain of the endoplasmic reticulum. *Plant Cell* **11**, 2167-2185.

Mullen, R. T., Flynn, R. and Trelease, R. N. (2001). How are peroxisomes formed? The role of the endoplasmic reticulum and peroxins. *Trends Plant Sci.* **6**, 256-261.

Newcomb, E. H., Tandon, S. R. and Kowal, R. R. (1985). Ultrastructural specialization for ureide production in uninfected cells of soybean root-nodules. *Protoplasma* **125**, 1-12.

Oksanen, E., Häikiö, E., Sober, J. and Karnosky, D. F. (2003). Ozone-induced H_2O_2 accumulation in field-grown aspen and birch is linked to foliar ultrastructure and peroxisomal activity. *New Phytol.* **161**, 791-799.

Pais, M. S. and Feijó, J. A. (1987). Microbody proliferation during the microsporogenesis of *Ophrys lutea* Cav. (Orchidaceae). *Protoplasma* **138**, 149-155.

Palma, J. M., Garrido, M., Rodríguez-García, M. I. and del Río, L. A. (1991). Peroxisome proliferation and oxidative stress mediated by activated oxygen species in plant peroxisomes. *Arch. Biochem. Biophys.* **287**, 68-74.

Passreiter, M., Anton, M., Lay, D., Frank, R., Harter, C., Wieland, F. T., Gorgas, K. and Just, W. W. (1998). Peroxisome biogenesis: Involvement of ARF and coatomer. *J. Cell Biol.* **141**, 373-383.

Rottensteiner, H., Stein, K., Sonnenhol, E. and Erdmann, R. (2003). Conserved function of Pex11p and the novel Pex25p and Pex27p in peroxisome biogenesis. *Mol. Biol. Cell* **14**, 4316-4328.

Sakai, Y. and Subramani, S. (2000). Environmental response of yeast peroxisomes. *Cell Biochem. Biophys.* **32**, 51-61.

Sakai, Y., Marshall, P. A., Saiganji, A., Takabe, K., Saiki, H., Kato, N. and Goodman, J. M. (1995). The *Candida boidinii* peroxisomal membrane protein Pmp30 has a role in peroxisomal proliferation and is functionally homologous to Pmp27 from *Saccharomyces cerevisiae*. *J. Bacteriol.* **177**, 6773-6781.

Schrader, M. and Fahimi, H. D. (2004). Mammalian peroxisomes and reactive oxygen species. *Histochem. Cell Biol.* **122**, 383-393.

Schrader, M., Baumgart, E., Volkl, A. and Fahimi, H. D. (1994). Heterogeneity of peroxisomes in human hepatoblastoma cell-line Hepg2-evidence of distinct subpopulations. *Eur. J. Cell Biol.* **64**, 281-294.

Schrader, M., Reuber, B. E., Morrell, J. C., Jimenez-Sanchez, G., Obie, C., Stroh, T. A., Valle, D., Schroer, T. A. and Gould, S. J. (1998). Expression of PEX11β mediates peroxisome proliferation in the absence of extracellular stimuli. *J. Biol. Chem.* **273**, 29607-29614.

Schrader, M., Wodopia, R. and Fahimi, H. D. (1999). Induction of tubular peroxisomes by UV irradiation and reactive oxygen species in HepG2 cells. *J. Histochem. Cytochem.* **47**, 1141-1148.

Seki, M., Carninci, P., Nishiyama, Y., Hayashizaki, Y. and Shinozaki, K. (1998). High-efficiency cloning of *Arabidopsis* full-length cDNA by biotinylated CAP trapper. *Plant J.* **15**, 707-720.

Seki, M., Narusaka, M., Kamiya, A., Ishida, J., Satou, M., Sakurai, T., Nakajima, M., Enju, A., Akiyama, K., Oono, Y. et al. (2002). Functional annotation of a full-length *Arabidopsis* cDNA collection. *Science* **296**, 141-145.

Smith, J. J., Marelli, M., Christmas, R. H., Vizeacoumar, F. J., Dilworth, D. J., Ideker, T., Galitski, T., Dimitrov, K., Rachubinski, R. A. and Aitchison, J. D. (2002). Transcriptome profiling to identify genes involved in peroxisome assembly and function. *J. Cell Biol.* **158**, 259-271.

Tam, Y. Y. C., Torres-Guzman, J. C., Vizeacoumar, F. J., Smith, J. J., Marelli, M., Aitchison, J. D. and Rachubinski, R. A. (2003). Pex11-related proteins in peroxisome dynamics: a role for novel peroxin Pex27p in controlling peroxisome size and number in *Saccharomyces cerevisiae*. *Mol. Biol. Cell* **14**, 4089-4102.

Tanaka, A., Okumoto, K. and Fujiki, Y. (2003). cDNA cloning and characterization of the third isoform of human peroxin Pex11p. *Biochem. Biophys. Res. Commun.* **300**, 819-823.

Thoms, S. and Erdmann, R. (2005). Dynamin-related proteins and Pex11 proteins in peroxisome division and proliferation. *FEBS J.* **272**, 5169-5181.

Titorenko, V. I. and Rachubinski, R. A. (2001). Dynamics of peroxisome assembly and function. *Trends Cell Biol.* **11**, 22-29.

Titorenko, V. I. and Rachubinski, R. A. (2004). The peroxisome: orchestrating important developmental decisions from inside the cell. *J. Cell Biol.* **164**, 641-645.

Trelease, R. N. (2002). Peroxisomal biogenesis and acquisition of membrane proteins. In *Plant Peroxisomes* (ed. A. Baker and I. A. Graham), pp. 305-335. Netherlands: Kluwer Academic Publishers.

Trelease, R. N. and Lingard, M. J. (2006). Participation of the plant ER in peroxisomal biogenesis. In *The Plant Endoplasmic Reticulum* (Plant Cell Monographs) (ed. D. G. Robinson). Heidelberg, Germany: Springer-Verlag. In Press.

Veenhuis, M., Salomons, F. A. and van der Klei, I. J. (2000). Peroxisome biogenesis and degradation in yeast: a structure/function analysis. *Microsc. Res. Tech.* **51**, 584-600.

Veenhuis, M., Kiel, J. A. K. W. and van der Klei, I. J. (2003). Peroxisome assembly in yeast. *Microsc. Res. Tech.* **61**, 139-150.

Vizeacoumar, F. J., Torres-Guzman, J. C., Tam, T. T. C., Aitchison, J. D. and Rachubinski, R. A. (2003). *YHR150w* and *YDR479c* encode peroxisomal integral membrane proteins involved in the regulation of peroxisome number, size, and distribution in *Saccharomyces cerevisiae*. *J. Cell Biol.* **161**, 321-332.

Vizeacoumar, F. J., Torres-Guzman, J. C., Aitchison, J. D. and Rachubinski, R. A. (2004). Pex30p, Pex31p, and Pex32p form a family of peroxisomal integral membrane proteins regulating peroxisome size and number in *Saccharomyces cerevisiae*. *Mol. Biol. Cell* **15**, 665-667.

Wanner, G. and Theimer, R. R. (1978). Membranous appendices of spherosomes (oleosomes)-possible role in fat utilization in germinating oil seeds. *Planta* **140**, 163-169.

Yamamoto, K. and Fahimi, H. D. (1987). Three-dimensional reconstruction of a peroxisomal reticulum in regenerating rat liver: evidence of interconnections between heterogeneous segments. *J. Cell Biol.* **105**, 713-722.

Yan, M., Rayapuram, N. and Subramani, S. (2005). The control of peroxisome number and size during division and proliferation. *Curr. Opin. Cell Biol.* **17**, 1-8.